

THE STRENGTH AND MODE OF FAILURE OF A SQUARE DUCT ENTERING A SQUARE PLATE UNDER INTERNAL PRESSURE, BY EXPERIMENT, CLASSICAL AND NON-LINEAR FINITE ELEMENT ANALYSIS ©

G. Norton B.Sc.* , D.F. Pilkington Ph.D. B.Sc(Eng)** , J.B. Carr M.Sc. C.Eng**

* Health and Safety Executive, HSE, ** Salford University Business Services Ltd., SUBSL.

Process plant used to handle powders or any other materials which could cause a dust explosion are generally protected by the inclusion of venting panels. The accurate design of venting panels requires knowledge of the structural strength of the process plant being protected. A theoretical method of predicting this strength has been developed by Production Engineering Research Association (PERA) but it was thought necessary to validate the method by experimental work. This paper considers the PERA equations relating to square ducts entering square plates. Initial testing has indicated that failure of such a complex structure requires an equation to represent the interaction of the two constituent parts, namely the square duct and the plate with a square hole.

In order to develop such an equation, classical geometric consideration have been applied by SUBSL together with non-linear finite element analysis carried out by HSE. These analyses have provided valuable information on how to proceed with developing an equation to represent the strength of duct/plate joints. Perhaps of more interest, it has led to a different design philosophy which may strengthen such joints.

Keywords: Strength of weak vessels, high rate of pressure rise, non-linear finite element analysis, large displacements of square ducts under pressure, testing of square duct-plate joints.

1. INTRODUCTION

In another paper presented at this conference, (1), a full resume of the background to this work has been given.

The PERA approach to this complex problem of the strength of weak pressure vessels was to identify a range of common features of dust handling plant, analyse how they would distort under overpressure conditions, and calculate a strength factor for the particular feature. By rating the strength of all features in a complete vessel, the weakest point can be identified and the vessel itself rated accordingly.

The PERA approach to assessing the strength of weak pressure vessels produced much interest among the contributors to the project. Because of the novelty of some of the ideas, however, validation by a suitable programme of experimental work was considered necessary.

One feature of weak vessels considered by PERA is that of circular or rectangular ducts entering circular or rectangular flat plates. PERA give suggestions on how to reinforce such a duct/plate joint, using reinforcing 'rings' but do not give a method of estimating the strength of an existing joint. This is the objective of the current work.

The worst geometric combination of a duct/plate joint was considered to be that of a square duct entering a square plate, fig 1, and it is this combination which is considered here. The individual strengths of the duct and plate have to be considered as well as their interaction. Simple square ducts have been investigated using static pressure testing and finite element analysis and an equation for the deformation of a square duct under internal pressure has been developed. Using this information, finite element analysis and dynamic pressure testing of duct-plate intersections were then carried out using the test rig described in (1).

2. NON-LINEAR FINITE ELEMENT ANALYSIS

Linear finite element analysis, FEA, is commonly used to calculate displacements and the resultant stresses within loaded components. Inherent in linear FEA are the assumptions that any displacements will be small compared with the component size and that the resulting stresses will be below the yield stress of the material. As displacements increase and stresses exceed yield then the results obtained from linear FEA become increasingly inaccurate. To analyse components where such excessive displacements or stresses occur then non-linear FEA must be used. Such problems fall into two distinct areas:

- 1) Geometric non-linearity where the displacements of the structure under load directly change the applied loading system - e.g. very flexible components; and,
- 2) Material non-linearity where displacements produce stresses which are greater than the yield stress of the component material.

In many non-linear situations, both conditions occur together.

In non-linear FEA the load is applied in steps, the stiffness of the component being recalculated at each step to take account of its deformed shape and the elastic/plastic state at the end of the previous load increment. This automatically implies long total solution times and requires large storage capacity in order to store the full load history of the problem. The structures under consideration here sustained large and permanent deformations and therefore require non-linear FEA.

3. STRENGTH OF SQUARE PLATES

Little experimental work has been conducted on fully restrained square plates under pressure but sufficient theoretical knowledge, based on circular plates (1), is available to model their behaviour. The case of a square plate with a square hole would appear impossible to test on its own due to the difficulty in simulating the correct loading around the hole in order to represent a

duct. No geometric formulation appears possible and only non-linear FEA has been considered.

3.1 PERA Equation

For a complete square plate, assuming fully restrained edges of length a , the PERA equation in its simplest form is :-

$$P = 9.8 \frac{\sigma_{YIELD} t}{a} \epsilon^{0.5} \quad (i)$$

where

- P = the applied pressure
 σ_{YIELD} = the material yield stress
 t = the plate thickness

This assumes a maximum allowable value of strain (ϵ) which allows the plate to bulge. The resulting membrane stresses at yield are in equilibrium with the applied pressure. The allowable strain is subject to many interpretations but currently a strain value of 0.02, or 2% is favoured for all ductile materials.

PERA suggests this formula can be used where reinforcing of holes is designed to their recommendations. A parameter which is not considered in this approach is the ratio of hole size to plate size. As this approaches unity the plate becomes less important.

3.2 Finite Element Analysis

A complete square plate has not been analysed as work conducted on circular plates is relevant and can be applied. The square plate with a square hole is currently being analysed with correct loading, normal to the plate as would be applied by a duct, around the hole boundary. Initial work has indicated that the stresses induced at the corner of the hole have a maximum tensile value at 45 degrees to the edge of the hole. A simple consideration of the loading would also identify the maximum stress in this direction and position.

4. STRENGTH OF SQUARE DUCTS

4.1 PERA Approach

Each individual side of the duct is considered as a rectangular plate and given a corresponding strength. For ducts, the PERA equation for infinitely long plates would be more applicable. In its simplest form this is :-

$$P = 4.9 \sigma_{\text{YIELD}} \frac{t}{a} \epsilon^{0.5} \quad (\text{ii})$$

This approach assumes that the edges are fully restrained against in-plane movement. It is not difficult to appreciate that this assumption is invalid because a square duct will deform to become circular and in the process the corners will move inwards.

4.2 Initial Static Pressure Test Results

Work was undertaken on a simple 300 mm square duct, 1500 mm long, made from 22 swg mild steel. The specimen contained two longitudinal butt welds down the centre line of two opposite sides. Fig 2 shows the design of the specimen with the ends of the duct folded around, and welded to, angle iron 'rings' which locally maintains the duct cross-section. The specimen was bolted directly to the test bed and blanked off with a 12 mm thick plate. The specimen was subjected to static pressure testing with displacements being measured at the centre of each face of the duct. Very low pressures were required to produce relatively large displacements and a simple water manometer was used to measure the pressure. A maximum pressure of 0.5 bar was applied, at which load the central section was essentially circular.

4.3 Classical Analysis

From the pressure versus deflection data obtained for the simple square duct, it was obvious that the duct wanted to form a circular cross-section at very low pressures. For such deformations, until the duct becomes circular, the only stress system possible to satisfy equilibrium is bending. In bending, the duct cross-section would deform at very low pressure, as the bending stiffness of the duct material is extremely small. This deformation is an obvious case of geometric non-linearity. Visual inspection of the test specimen indicated that plastic hinges formed, at low pressure, very close to the corners. At half a bar pressure the duct, at mid span, had effectively become circular and maintained this shape when the pressure was removed. This indicated that plasticity was also involved at very low pressures. With the following assumptions it is possible to develop a very simple relationship between the displacement of the duct side and the internal pressure :-

- 1) the duct is infinitely long and a cross-section of the duct can be treated as a beam system,
- 2) each side deforms into part of a large cylinder, whose radius R, reduces with pressure load until an equivalent cylinder is formed having the same perimeter length as the original square section,
- 3) plastic hinges form at the corners and the resulting internal moment, M_p , is constant; and,
- 4) the internal moment at other locations, away from the corners, can be calculated using the Engineers Theory of Bending, in terms of the curvature. (If this is greater than M_p then the plastic moment is used.)

A section of one side plate of the square duct, thickness t and unit width, is shown in its assumed deformed shape in Fig 3. The internal forces generated at the corner and on the centre line are given and satisfy force equilibrium for the applied internal pressure, P . The internal moments at the ends both act clockwise as drawn and the overall moment equilibrium for the deformed geometry gives the following relationship for pressure in terms of the parametric co-ordinate, θ . The central displacement, δ , is also given in terms of θ so that the resulting curve for pressure versus central displacement can be generated.

$$P = \frac{M_p + M}{R^2 \sin^2(\theta/2) (\cos \theta - \sin \theta)} \quad (\text{iii})$$

$$L = 2R\theta \quad (\text{iv})$$

$$\delta = 2R \sin^2(\theta/2) \quad (\text{v})$$

$$M_p = \sigma_{\text{YIELD}} t^2 / 4 \quad (\text{vi})$$

$$M = E t^3 / 12 R \quad \text{or} \quad M_p \text{ whichever is the smaller} \quad (\text{vii})$$

where

$$E = \text{Young's modulus}$$

Notice that as the duct deforms the corners actually move inwards along a line at 45 degrees to the original position of the sides.

4.4 Finite Element Analysis

All the non-linear FEA was undertaken by HSE, the package used being NISA, running on a stand-alone Sun Sparcstation 2 workstation. Two models were developed representing the 1500 mm long, 300 mm square ducts. The first was a simple model for comparison with the classical formulation for an infinite length duct. A single element across the width was used to model the cross-section. The second model was a full model using the actual length of the duct as tested. Full advantage was taken of symmetry to minimise the size of the model, with appropriate boundary conditions being applied. Both models used general 8-noded quadrilateral shell elements.

The material was assumed to be elastic-perfectly plastic with material properties corresponding to mild steel, that is,

| | | | |
|-----------------|-------------------------|---|--------------------------|
| Youngs Modulus, | E | = | 210000 N/mm ² |
| Poissons Ratio, | ν | = | 0.3 |
| Yield stress, | σ_{YIELD} | = | 300 N/mm ² |

Pressure was applied to the inside of the duct in a series of steps up to a maximum of 0.5 bar.

Fig 4 shows the finite element solution for central side displacement against pressure, compared with the classical solution using the equations given in Section 4.3. This is for the infinitely long duct. The duct stiffness increases dramatically at θ equals 45 degrees, when the square duct becomes circular.

Fig 5 shows the experimental displacement versus pressure result compared with the corresponding FEA curve for the finite duct length. For the 300 mm square duct the limiting central displacement is 41 mm, when the duct becomes circular. This represents the actual movement of the centre relative to its original position. Further displacement is not possible in bending and, for low pressures where tensile membrane strains can be ignored, this displacement is the limit to which calculated solutions and experimental work must be asymptotic.

A model of the finite length duct is currently being investigated by non-linear FEA but with the cross-section at the centre of its length restrained against in-plane movement. This has indicated that very large restraining forces are required, essentially at the four corners only, to maintain the square cross-section.

4.5 Discussion of Results

Fig 4 shows the variation of central side displacement with pressure for an infinitely long mild steel duct with a wall thickness of 0.71 mm, (22 swg). Predictions for both finite element analysis and the classical equation are given. Both sets of results are for an assumed material yield stress of 300 N/mm². Agreement between the two is extremely good, with both solutions tending to the asymptotic displacement value of 41 mm at low pressures. The effect of plastic hinges which develop in the corners is very easy to see both from the FEA plots and by examination of the deformed test specimen. The solution as presented for the classical analysis does not consider the initial linear elastic behaviour, at very low pressure, but this is given in (2).

Fig 5 compares the measured central side displacements in the finite length duct with those obtained by FEA. The displacements from the test were obtained by averaging the measured displacements at mid length for the four sides of the duct. Again, the comparison is very good. The irregularity at the lower end of the pressure range is due to one side of the specimen 'oil canning'. This is a sudden change of deflection as the panel jumps from one stable state through to another. This behaviour only occurs at low load and, once it has occurred, the deflections become more regular.

At higher pressures the FEA results indicate lower stiffnesses than those measured in the experiments. This is due in part to the material properties being modelled as elastic-perfect plastic, whereas for steel the stress will continue to increase with increasing strain.

Comparing Fig 4, the infinite length case, with Fig 5, the finite length case, indicates a significant stiffening in the finite length specimen, suggesting the finite length has an appreciable restraining effect on the central displacement. Since this observation was made, reference to

photographic evidence has verified that there is no flattening of the curve of sectional central displacement over the length of the duct. This confirms that even at the centre of the finite length duct, displacement is being limited by the duct ends and the circular cross-section is not being attained. The reason for this is that as the duct ends are square the longitudinal loads restrain the central section against deformation.

The strength of the square duct can not be calculated by considering the sides independently but could be considered in its circular form, provided it is not restrained against cross-section deformation. Longitudinal joints in the duct can be considered in the circular form. Any restraint, e.g. flanged joints, will involve analysis similar to that required for the duct-plate intersection. Initial FEA on a centrally restrained square duct indicates large forces are necessary to prevent deformation, nominally in the vicinity of the corners. In the duct-plate structure it is the plate which has to provide such restraining forces.

5. STRENGTH OF DUCT-PLATE JOINTS

This work has been undertaken in order to provide a method for assessing the strength of duct-plate joints. The strength of such a joint has to be considered together with the individual strengths of the duct and the plate. No analysis of the combined structure is offered at this time.

5.1 PERA Approach for the Strength of Duct-Plate Joints

The PERA equations do not include a method for estimating the strength of an existing duct-plate joint. However, for design purposes, there are suggestions on how to reinforce the intersection by fastening a reinforcing 'ring' around the joint. The reinforcing structure is designed to the following concepts :-

- 1) the cross-sectional area of the 'ring', A is based on the greatest cross-sectional side length, a , of the duct and on the thickness of the plate, t ;

$$\text{where } A = \frac{a t}{2} \quad (\text{viii})$$

- 2) the material is distributed in such a way that the maximum thickness of the reinforcing ring is less than seven times the thickness of the plate.

The reinforcing effectively replaces the material removed from the plate, and positions it close to the remaining plate material. The reinforced plate is then rated as a complete, virgin plate allowing other PERA equations to be used.

The duct is assumed to be unaffected by the joint and is rated as a separate structure.

In the case of circular plates and circular ducts this approach may be valid, but it has not

been investigated in previous or current experimental programmes. The case of plates with square ducts was believed to present far more difficulties than addressed by the PERA design considerations. An experimental programme was undertaken testing square duct-plate 'joints' both with and without reinforcing to the PERA recommendations.

5.2 Experimental Tests

Specimens were manufactured from 22 swg mild steel, with 300 mm square ducts, 1000 mm long, welded into 1000 mm square plate. Specimens with and without reinforcing of the joint, to the PERA recommendations, were tested to establish the failure mode of the joint. Fig 6 shows the design of the duct-plate specimens and how the plate edges are held to produce 'zero' in-plane movement. The plate edges of the specimens were bolted to the test bed, over the central 600 mm hole in the rig, but raised above the bed on 25 mm packing pieces to maximise the effects of pressure on the plate. The duct cross-section was identical to that used in the simple duct specimens tested. The top of the duct was welded to a reinforcing structure to locally maintain the duct cross-section. This end was blanked off with a 12 mm thick plate. For the duct-plate specimens progressive testing was used, without knowing whether it was valid, in order to establish the mode of failure. The duct used in the static testing was later tested dynamically to 0.5 bar and did not exhibit any significant further distortion. Since these tests were done, more work has shown progressive testing to be acceptable. Progressive testing has been discussed in (1), where it was found to be representative of a single test to the same pressure.

The unreinforced specimens exhibited small local failures at all corners with the duct pulling away from the plate at 0.5 bar. A further test at 0.75 bar resulted in the duct pulling further away from the plate, with the plate itself showing signs of failure along the diagonals from each of the duct corners, see fig 7. Further testing resulted in total failure of the specimen at the joint at 1.5 bar.

The reinforced specimen did not show any local failure until a pressure of 1 bar, when the duct pulled away from the reinforcing on the plate, which remained fixed to the plate. Total failure of this specimen then occurred at a pressure of 1.4 bar. One reinforced specimen was tested to failure as a single test. Failure occurred at a pressure of 1.6 bar.

5.3 Finite Element Analysis

The results of FEA on a full model of the duct-plate joint indicated large stress concentrations at the corners of the joint. This suggests that failure of the duct-plate intersection would start at the corner of the joint with the duct pulling from the corner. This was confirmed experimentally and gave a good insight into the experimental mode of failure. Although the ensuing crack development could possibly be modelled, very little extra knowledge would be gained.

5.4 Discussion of Results

In the tests, failure was always initiated from the corner of the intersection for both the reinforced and unreinforced specimens. Initially the duct pulled away from the plate at the corner, pulling inwards to try to form a circular cross-section. The plate also bulged, allowing the centre of the duct sides to move out as the duct went circular.

The analysis of the square duct has shown that large deformations will take place at low pressures, this indicates that for an intersection between a square duct and a plate the initial failure will be the duct pulling away from the plate in the corners. The plate will eventually split symmetrically at the corners perpendicular to the initial failure. This can be seen from fig 7, a photograph of a cracked specimen.

The FEA for the duct restrained at mid-section, shows that large corner loads are generated at the restraint. At the joint with the plate, the plate will supply equivalent restraint, resulting in large tensile stresses at the corners in the vicinity of the initial failure as seen in testing. From the tests it was observed that the diagonal cracking of the plate at the corners occurs as a secondary failure once cracking between the duct and the plate has already occurred.

6. CONCLUSIONS

The feature of a square duct entering a square or circular plate cannot be analysed in the manner proposed in the PERA equations. Both experimental testing and non-linear FEA indicate a mode of failure not considered by PERA. The actual mode of failure initiates at the corner of the duct-plate joint as the duct pulls away from the plate as it tries to form a circular cross-section. For this reason it is felt better to reinforce the duct to maintain its square cross-section rather than to strengthen the plate. If this can be done then the plate itself is automatically reinforced against tensile failure in the corner.

Further FEA and experimental work is being considered in order to identify the best way to reinforce such joints. Current thoughts are to consider some form of curved gusseting at the corners. This would help to maintain the cross-section of the duct at the plate but allow some duct movement away from the plate.

More work is also proceeding in an attempt to calculate the tensile stresses generated at the corners in order to predict initiation of failure. This condition could be defined as failure for this feature.

The combination of experimental work, classic analysis and non-linear finite element analysis has again demonstrated the effectiveness of such an approach to the understanding of a very complex structural feature. The final objective of developing an equation to predict the strength of the joint has not yet been attained but this should be accomplished in the future. This investigation has highlighted the complex behaviour of features in weak vessels under internal pressure.

The PERA equations represent an initial approach for vessel rating, but require extending and modifying in the light of experimental results. Ultimately it is hoped that this work will contribute to the development of a guide to assist in the design of weak pressure vessels.

REFERENCES

1. D.F. Pilkington et al, Hazards XII Conference 1994, Design and development of a rig for the pressure testing of weak pressure vessels etc
2. Stephen Timoshenko, 1940, Theory of Plates and Shells - McGraw Hill

UNITS

$$1 \text{ bar} = 0.1 \text{ N/mm}^2$$

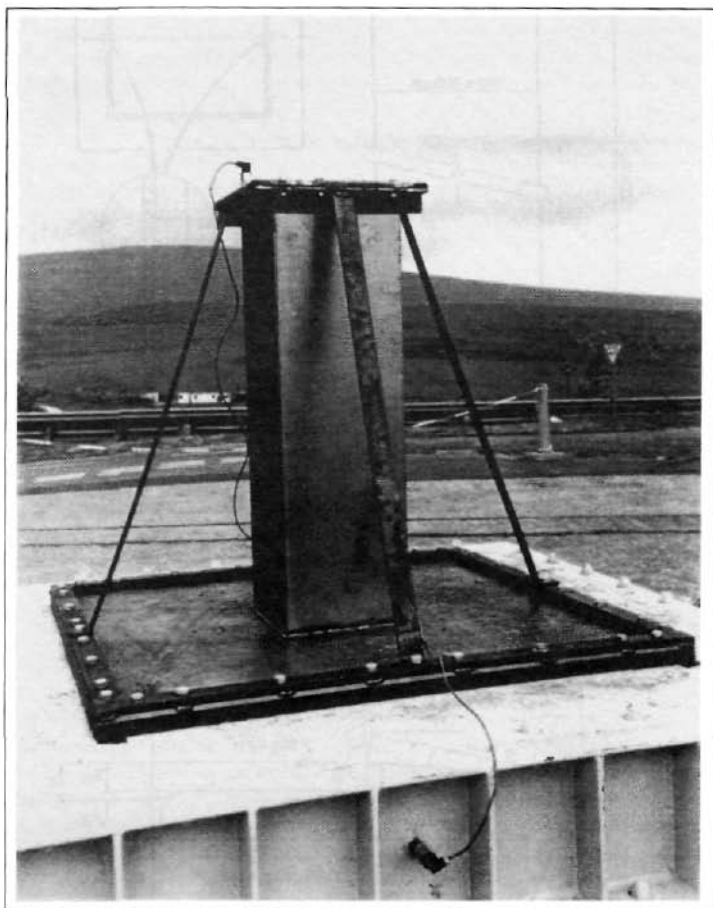


Fig.1 - Photograph of a square duct-plate specimen.

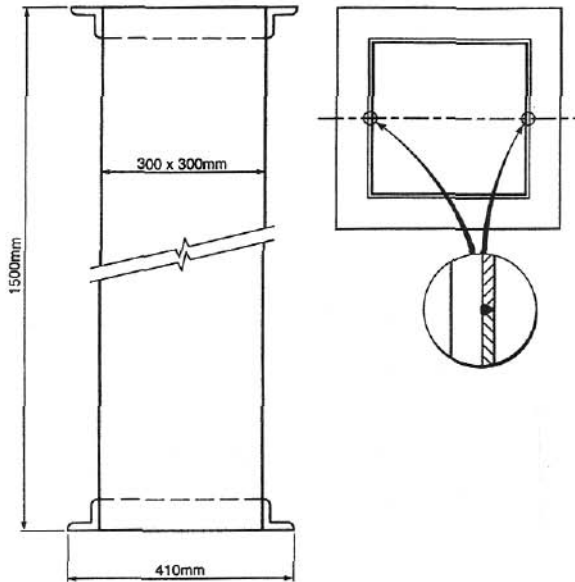


Fig.2 - Schematic drawing of a duct specimen.

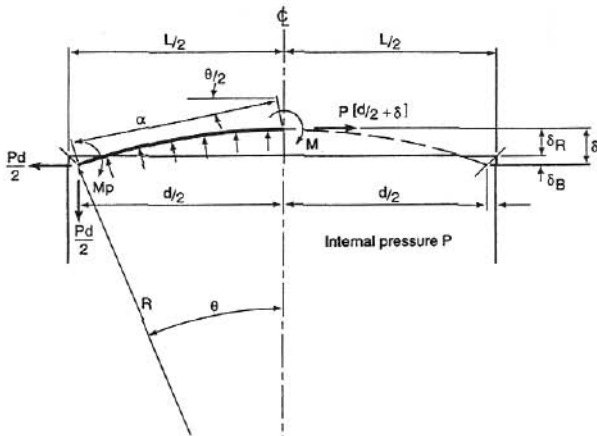


Fig.3 - Section through a duct side under pressure loading, showing assumed deformed shape.

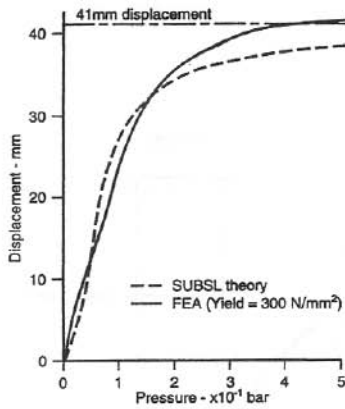


Fig.4 - Comparison of central side displacement of a pressure loaded infinitely long duct as predicted by finite element analysis and as calculated using the derived equation.

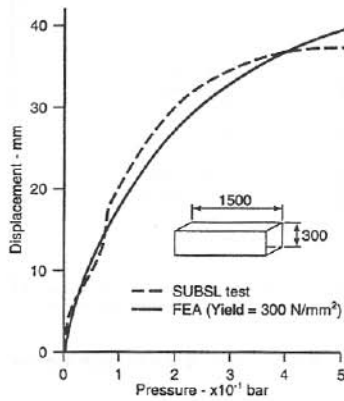


Fig.5 - Comparison of central side displacement of a pressure loaded 1.5m long duct as predicted by finite element analysis and as measured in tests.

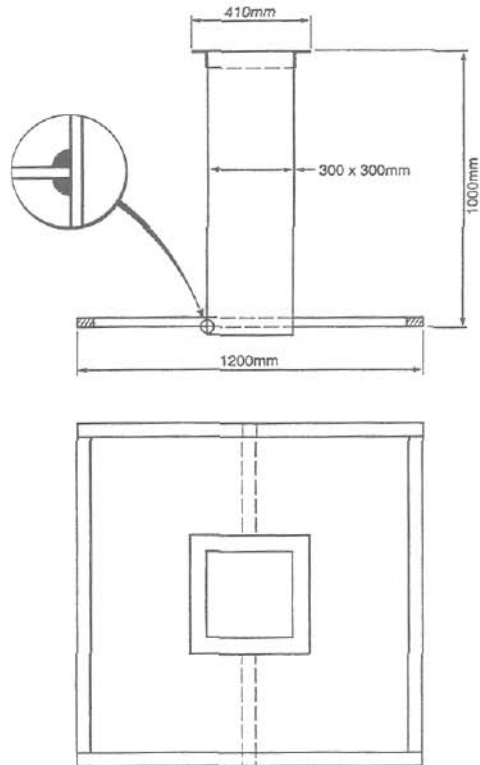


Fig.6 - Schematic drawing of a duct plate specimen.

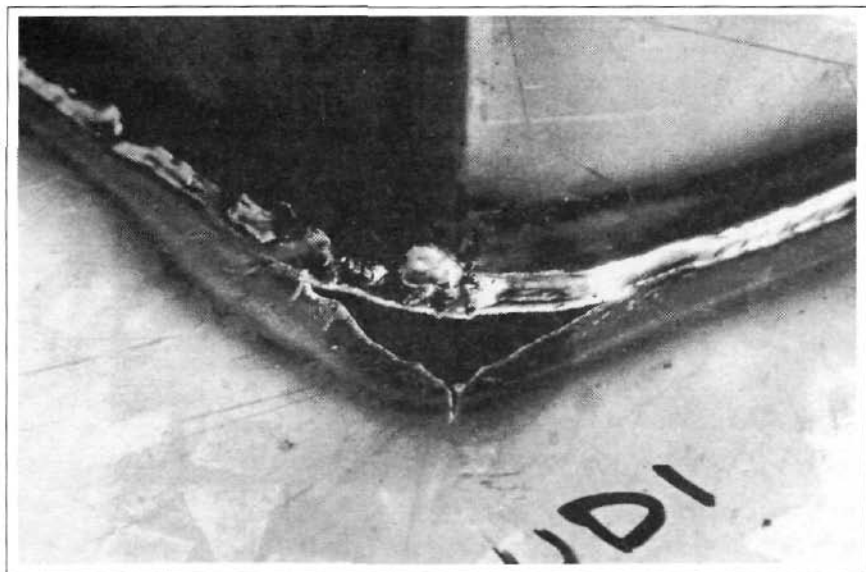


Fig.7 - Photograph showing the mode of failure of a duct-plate joint.